

## Mean-field calculations of the properties of the dilute $t$ - $J$ model for high-temperature superconductivity

J. W. Halley, X-F Wang, and S. Davis

*School of Physics and Astronomy, University of Minnesota, Minneapolis, Minnesota 55455*

(Received 5 March 1992)

We describe mean-field calculations of the properties of the dilute  $t$ - $J$  model for high- $T_c$  superconductors. We first discuss a physical motivation for the model in terms of the effects of oxygen vacancies and the appropriate parametrization for a qualitative description of high- $T_c$  superconductors. We briefly review our mean-field numerical methods. We present results on the density of states, local carrier density, the transition temperature as a function of carrier concentration, oxygen-vacancy concentration, and elastic-scattering impurity concentration, as well as the dc conductivity. These are compared with experiment on high- $T_c$  materials. We conclude that the model is a promising framework for understanding high- $T_c$  materials microscopically.

### INTRODUCTION

A conspicuous feature of the copper oxide superconductors,<sup>1,2</sup> which is often assumed to be an inessential complication by theorists, is that virtually all of the high-temperature superconducting materials have a very high degree of spatial disorder,<sup>3-5</sup> leading to mean free paths which are at best a few times the superconducting coherence length. This means at least that one should be developing theoretical methods and models that take account of the microscopic disorder. There is also a possibility<sup>6,7</sup> that some kinds of point defects or twin boundaries might act like "pairing centers" and enhance the pairing interactions, leading to the superconductivity itself. In this paper we will present a qualitative rationale for a dilute  $t$ - $J$  model as a description of the possible effects of oxygen vacancies in the copper oxygen planes of high- $T_c$  materials and give mean-field numerical results for the density of states, transition temperature, local charge density, and conductivity arising in the model. Finally, we will compare the calculations with experiment.

### MICROSCOPIC MOTIVATION FOR THE DILUTE $t$ - $J$ MODEL

To motivate the model studied here (see also Refs. 8 and 9), we note that experiments show<sup>10</sup> that the carriers in hole-type high- $T_c$  superconductors are primarily (roughly 80%) oxygen like. Simplifying [Figs. 1(a) and 1(b)] to a model in which the holes are entirely oxygenlike in copper oxygen planes without defects, we next note that the exchange interaction between oxygen holes moving on the (square) lattice of oxygen sites in the copper oxygen planes in the absence of vacancies is expected to be small and we neglect it. Now consider the possible effects of oxygen vacancies in the plane. (We make a distinction, as a few authors do not, between holes and vacancies here. A vacancy is a missing oxygen atom. A hole is an oxygen atom with charge 1- instead of 2-.) As discussed by many authors,<sup>11</sup> an oxygen vacancy is expected to bind two screening electrons, residing mainly at

the copper ions on each side of the vacancy, thus rendering the valency of those copper ions approximately 1+. A free hole propagating through the lattice on the oxygen ions can approach this charge-neutral vacancy without Coulomb penalty and mix with a hole on one of the two  $\text{Cu}^{1+}$  ions next to it without expending energy  $U$  (because

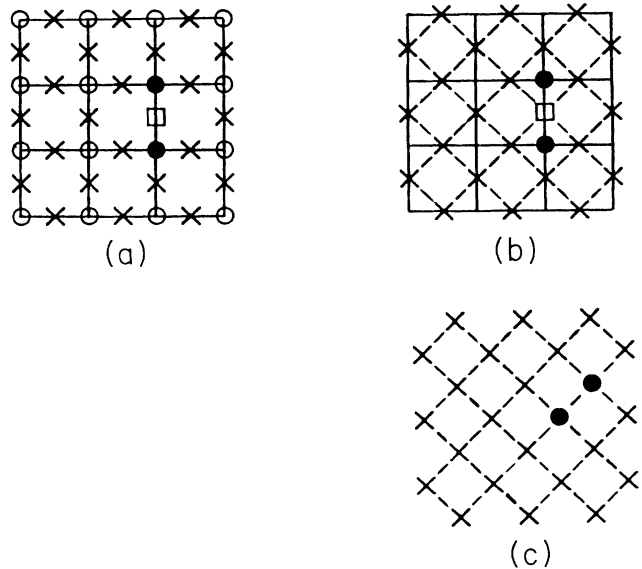


FIG 1. Sketch of the  $\text{CuO}_2$  plane: (a) Model, including detailed geometrical structure of the plane and both oxygen and copper ions. Open circles are copper ions with valency 2+. Solid circles are copper ions with valency 1+. Crosses are oxygen ions. Square is an oxygen vacancy. (b) First stage of simplification of the model. All copper ions except those with valency 1+ next to oxygen vacancies are neglected. (c) Second stage of simplification. The local geometry around a vacancy is altered so that the copper ions with valency 1+ lie on the same square lattice as the oxygen ions. The oxygen vacancy is replaced by a special bond, at which the exchange interaction is finite. The value of the on-site energy of the two site neighbors of these special bonds is different from zero, corresponding to their chemical origin in the original model as copper sites.

the copper is cuprous). Thus holes will attain a larger  $d$ -orbital character as a consequence of the presence of oxygen vacancies. If one imagines that a second hole migrates to the second copper adjoining the vacancy (overcoming the Coulomb barrier due to the first hole), then the two copper holes will interact with an exchange interaction across the space between them (which is empty of atoms because the oxygen is missing). The resulting exchange interaction  $J$  is obviously not the same as the exchange interaction between copper sites in the usual  $t$ - $J$  model, and its magnitude is not known. We assume here that this exchange  $J$  coupling copper spins on copper sites adjacent to oxygen vacancies is large. With these assumptions we obtain a dilute  $t$ - $J$  model as sketched in Fig. 1(b). Carriers attain a copper character only at copper sites adjacent to oxygen vacancies and are coupled only there. Without losing any essential qualitative features, we simplify to the following slightly simpler model [Fig. 1(c)]: Carriers move with nearest-neighbor hopping on a square lattice with exchange interaction  $J$  between a randomly selected fraction  $p$  of the bonds. The on-site energy, called  $\varepsilon$  at these special bonds, is allowed to be different from that at the other sites. We also neglect the single-occupancy constraint in the model studied here. This is not strictly consistent, but we have shown elsewhere by use of variational Monte Carlo calculations<sup>8,9</sup> that it does not affect our qualitative conclusions concerning the nature of the ground state in the model.

These considerations lead to the Hamiltonian

$$\begin{aligned}
 H - \mu N = & \sum_{i,\sigma} (\varepsilon_i - \mu) d_{i,\sigma}^\dagger d_{i,\sigma} + \sum_{i,j,\sigma} (b_{ij} d_{i,\sigma}^\dagger d_{j,\sigma} + \text{H.c.}) \\
 & - \sum_{i,j} (J_{ij}/2)(d_{i\uparrow}^\dagger d_{j\downarrow}^\dagger - d_{i\downarrow}^\dagger d_{j\uparrow}^\dagger) \\
 & \times (d_{j\downarrow} d_{i\uparrow} - d_{j\uparrow} d_{i\downarrow}) + \text{triplet terms} . \quad (1)
 \end{aligned}$$

We suppose that  $J_{ij}$  is zero except at a randomly selected fraction  $p$  of bonds where its value  $J_{ij} = J$  is a parameter of the model.  $b_{ij}$  is made the same at all nearest-neighbor pairs and set equal to  $b$ , a second parameter of the model. ( $b$  is more commonly called  $t$  in such models, but the latter symbol is reserved for the time here.)  $\varepsilon(i)$  is zero at sites away from special bonds, but finite and positive on sites next to special bonds. The value of  $\varepsilon$  at sites next to special bonds is a third parameter of the mode. Finally, the model must be studied as a function of the chemical potential  $\mu$ . The qualitative considerations outlined here suggest that, since the band described by the model is associated with electrons on the oxygen sites,  $\mu$  should lie near the top of the band. We do not have microscopic calculations of the magnitude of the  $J$  expected from these qualitative arguments and only note here that it will be affected by the fact that the copper ions relax toward each other and that the exchange is direct. The model described here is the same as that studied in Ref. 6, but the physical motivation is different, and partly for this reason the chosen parametrization discussed below is also different. In particular, we will choose the Fermi energy near the top of the band in order to describe a small number of holes as the carriers in the model.

In this paper we treat this model in BCS mean-field theory. The resulting superconducting state is one in which the pairing correlations induced by the sites with finite  $J$  extend across the sample at low enough temperatures or high enough concentration of sites with finite  $J$  in a manner reminiscent of percolation. The effects of the copper spins not near oxygen vacancies, including the possibility of antiferromagnetic order, are ignored.

## MEAN-FIELD METHODS

The mean-field methods used here take full numerical account of the disorder introduced by the point defects in the model. We define the retarded functions

$$\begin{aligned}
 G_\sigma^{ij}(t) &= i\Theta(t) \langle \{ d_{i,\sigma}(t), d_{j,\sigma}^\dagger(0) \} \rangle , \\
 F_\sigma^{ij}(t) &= -i\Theta(t) \langle \{ d_{i,\sigma}^\dagger(t), d_{j,-\sigma}^\dagger(0) \} \rangle .
 \end{aligned}$$

We obtain equations of motion for the functions  $G_{ij} = G_\uparrow^{ij} + G_\downarrow^{ij}$  and  $F_{ij}(t) = F_\uparrow^{ij} - F_\downarrow^{ij}$ :

$$\begin{aligned}
 i\hbar \frac{dG_{ij}}{dt} &= 2\hbar\delta(t)\delta_{i,j} + \varepsilon_i G_{ij} + \sum_\delta b_{i+\delta,i} G_{i+\delta j} \\
 &+ \sum_\delta (J_{i+\delta,i}/2)\Delta_{i,\delta} F_{i+\delta j} , \quad (2a)
 \end{aligned}$$

$$\begin{aligned}
 i\hbar \frac{dF_{ij}}{dt} &= -\varepsilon_i F_{ij} - \sum_\delta b_{i+\delta,i} F_{i+\delta j} \\
 &+ \sum_\delta (J_{i+\delta,i}/2)\Delta_{i,\delta}^* G_{i+\delta j} , \quad (2b)
 \end{aligned}$$

with the initial conditions  $G_{ij}(0) = -i2\delta_{ij}$  and  $F_{ij}(0) = 0$ . The gap equation is

$$\Delta_{ij}^* = -i \int_{-\infty}^{\infty} \frac{F_{ij}(\omega + i\varepsilon) - F_{ij}(\omega - i\varepsilon)}{e^{\beta\omega} + 1} d\omega , \quad (3)$$

where

$$F_{ij}(\omega + i\varepsilon) = \frac{1}{2\pi} \int_{-\infty}^{\infty} F_{ij}(t) e^{i(\omega + i\varepsilon)t} dt .$$

In order to reduce the number of equations, we define the sums  $F_i = \sum_j c_j F_{ij}$  and  $G_i = \sum_j c_j G_{ij}$ . Then  $F_i(0) = 0$  and  $G_i(0) = -i2c_i$ . To calculate<sup>6</sup> the average  $\Delta$  at the vacancy sites, we choose the  $c_i$  as follows. All  $c_i$  associated with sites not next to a vacancy are zero. Associate a random number  $\phi_i$  evenly distributed between 0 and  $2\pi$  with each site next to a vacancy. Now consider a pair of "copper" sites next to a vacancy. Label the sites 1 and 2. Set  $c_1 = e^{i\phi_2}$  and  $c_2 = e^{i\phi_1}$ . The phase factors  $e^{i\phi_i}$  are a calculational device only and are not to be confused with the phase factors associated with the gap function itself. Choosing  $c_i$  equal to zero away from vacancies is done only because we are choosing to evaluate  $\Delta$  self-consistently at those sites and does not mean that the gap is zero or neglected elsewhere on the lattice in our calculation.

With choices of the coefficients  $c_i$  described above, cancellation of random phases gives the gap equation: We define  $F_r(t) = \pm \sum_i \pm e^{-i\phi_i} F_i$ , where the plus sign is used if  $i$  is adjacent to an  $x$  bond and the minus sign is used if  $i$  is adjacent to a  $y$  bond. Then gap equation takes the

form

$$\Delta^* = \frac{-1}{2N_s\beta\hbar} \int_0^\infty \frac{F_r(t)}{\sinh(t\pi/\beta\hbar)} dt, \quad (4)$$

where  $N_s$  is the number of oxygen vacancies. By use of the preceding expressions, we obtain the equations of motion for  $F_i$  and  $G_i$ , which are essentially identical to the equation of motion written above.

We solve these equations by simple numerical integration in the time domain. In most of the calculations reported in this paper, we have used a realization of the model on a  $100 \times 100$  square lattice. To zeroth order (but not to first order), we will assume in the equations of motion that the magnitude of the gap is a fixed constant on the vacancy sites and zero otherwise. This zeroth-order assumption does not mean that the order parameter is zero away from the vacancies in our calculations, because the equations of motion above which we solve imply that the function  $F$  becomes nonzero away from vacancies if  $\Delta$  is finite at vacancies. This is a manifestation of the effect of propagation of the pairing order from one vacancy to the next which was discussed physically above. Numerical studies of the model when only two vacancy sites are present reveals that the model favors equal phases of the gap for vacancies on parallel bonds, but phases of the gap differing by  $\pi$  for vacancies on perpendicular bonds. These studies suggested that, in zeroth order, we choose the gap to be real and of one sign on the vacancies which are on bonds in the  $x$  direction and real and of the opposite sign on vacancies which are on bonds in the  $y$  direction. Calculations confirmed that this choice gives a more stable superconducting state than other choices of the phases  $\Delta$  in zeroth order. We could lift the assumption of a constant input magnitude of  $\Delta$  in more detailed calculations in this model without too much difficulty. In fact, the gap equation in our model is an integral equation, conveniently formulated in real space, and  $\Delta$  is a strong function of position in the lattice.

After a self-consistent solution for the average gap  $\Delta$  has been found using the methods outlined above, then the density of states can be found by essentially the same techniques: Define an amplitude

$$G_i(t) = \sum_j a_j G_{ij}(t). \quad (5)$$

The amplitudes  $a_j$  can be chosen in various ways depending on what quantity is of particular interest. The equation of motion is the same as that for  $G_{i,j}$  with initial condition

$$G_i(0) = -ia_i. \quad (6)$$

For example, we get the total density of states  $N(\omega)$  by setting

$$a_i = e^{i\phi_i}, \quad (7)$$

where  $\phi_i$  is a number chosen at random from the interval  $0 < \phi_i < 2\pi$  for each site  $i$ . The total density of states  $N(\omega)$  is then

$$N(\omega) = -\frac{1}{\pi} \text{Im} \left[ \int \sum_i e^{-i\phi_{i,\mu}} G_i(t) e^{i\omega t} dt \right]. \quad (8)$$

In principle, Eq. (8) is only true if one averages the right-hand side over phases, meaning that it is only exact if we calculate the right-hand side many times, choosing different sets of random numbers to associate with each site and orbital each time, and then average the result. On the other hand, experience has shown that for large samples just one set of randomly chosen phases gives a very accurate result. To get the local density of states defined as

$$N_i(\omega) = \sum_n |\langle i|n \rangle|^2 \delta(\omega - \epsilon_n), \quad (9)$$

we set

$$a_i = \delta_{l,i}, \quad (10)$$

where  $i$  is the site of interest. In these equations the ket  $|i\rangle$  is the tight-binding state localized at site  $i$  and the states  $|n\rangle$  are the eigenstates of the tight-binding problem in the (disordered) lattice. The local density of states is  $-(1/\pi) \text{Im} \int_{-\infty}^{\infty} G_i(t) e^{i\omega t} dt$ . Local charge densities are obtained by integrating the local density of states up to the Fermi level  $q_i = e \int_{-\infty}^{\mu} N_i(\omega) d\omega$ .

We discuss the numerical implementation of this method for calculating tight-binding densities of states in Ref. 11, where we also discuss the relationship of the method to other sparse-matrix methods.<sup>12,13</sup>

Finally, we can use the same methods to calculate the dc conductivity. Details are given elsewhere.<sup>14</sup> The conductivity of the normal state when the Fermi energy is  $E$  is given by

$$\sigma(E) = (\pi e^2 \hbar / L^d) \sum_{\alpha, \beta} |\langle \alpha | v^x | \beta \rangle|^2 \delta(E - E_\alpha) \delta(E - E_\beta), \quad (11)$$

where  $v^x$  is the current operator  $v^x = (1/i\hbar)[x, H]$  and  $L^d$  is the volume of the sample. We define

$$G_{p,q}(t) = \langle p | e^{-iHt} | q \rangle, \quad (12)$$

$$F_n^{(k)}(t) = \sum_m G_{n,m}(t) e^{i\phi_m^{(k)}}, \quad (13)$$

$$Z_n^{(k)} = \sum_p v_{p,n}^x e^{-i\phi_p^{(k)}}, \quad (14)$$

where  $\phi_p^{(k)}$  is random from  $0 < \phi_p^{(k)} < 2\pi$  and  $k=1,2$ . Then we introduce the two quantities

$$Q^{(1)}(E) = \sum_n Z_n^{(2)} \left[ \int F_n^{(1)}(t) e^{+iEt} \frac{dt}{2\pi} \right], \quad (15)$$

$$Q^{(2)}(E) = \sum_n Z_n^{(1)} \left[ \int F_n^{(2)}(t) e^{+iEt} \frac{dt}{2\pi} \right]. \quad (16)$$

Then the dc conductivity (at  $T=0$  K) is

$$\sigma(E) = \pi(e^2 \hbar / L^d) \langle Q^{(1)}(E) Q^{(2)}(E) \rangle, \quad (17)$$

where  $\langle \dots \rangle$  denotes the average over random phases. Many sets of random phases are needed for the calculation of the conductivity because the fluctuations in this calculation are only controlled by the number of sets of phases.

In the superconducting state, one has to include contributions<sup>15</sup> to the conductivity from the anomalous Green's functions  $F_{ij}(t)$  which characterize the Cooper pairs. Taking that into account, we find that the dc conductivity in the superconducting state is given as

$$\sigma^{\text{SC}}(E) = (\pi e^2 \hbar / L^d) \{ \text{Tr}[v^x G(E) v^x G(E)] + \text{Tr}[v^x F(E) v^x F^\dagger(E)] \}, \quad (18)$$

where

$$G_{ij}(E) = \int_{-\infty}^{\infty} e^{iEt} G_{ij}(t) \frac{dt}{2\pi}, \quad (19)$$

$$F_{ij}(E) = \int_{-\infty}^{\infty} e^{iEt} F_{ij}(t) \frac{dt}{2\pi}.$$

$L$  is the system size. To calculate  $\sigma^{\text{SC}}(E)$  numerically, we introduce two more quantities:

$$R^{(1)}(E) = \sum_n Z_n^{(2)} \left[ \int \sum_m F_{nm}(t) e^{i\phi_m^{(1)}} e^{+iEt} \frac{dt}{2\pi} \right]. \quad (20)$$

$$R^{(2)}(E) = \sum_n Z_n^{(1)} \left[ \int \sum_m F_{nm}(t) e^{i\phi_m^{(2)}} e^{+iEt} \frac{dt}{2\pi} \right]. \quad (21)$$

Then  $\sigma^{\text{SC}}(E)$  is obtained from

$$\sigma^{\text{SC}}(E) = (\pi e^2 \hbar / L^d) \langle Q^{(1)}(E) Q^{(2)}(E) + R^{(1)}(E) R^{(2)}(E) \rangle. \quad (22)$$

### SELECTION OF PARAMETERS FOR MODELING OF HIGH- $T_c$ SUPERCONDUCTORS

We set the parameter  $b$  (more commonly called  $t$ ) = 1 throughout, thus measuring energies in units of  $b$ . Thus the energy unit is of the order of 1 eV. The parameter  $\varepsilon$  is chosen so that the one-electron states on the sites next to the special bonds associated with finite  $J$  (and with oxygen vacancies in the physical interpretation) have diagonal energies near the top of the band. In our interpretation the band is predominantly oxygenlike, but the sites next to the special bonds are copperlike. Thus we may compare  $\varepsilon$  with  $\varepsilon_{pd}$ , recalling that we are working in an electron representation, but must bear in mind that, because the copper sites in question are next to oxygen vacancies, the value of  $\varepsilon$  would be expected to be lower than the value of  $\varepsilon_{pd}$ . The physical picture requires that  $\varepsilon < \mu$ ; otherwise, the oxygen vacancies would not be screened, as discussed in the Introduction. These arguments by no means fix the parameter  $\varepsilon$  uniquely. In most of the results presented in the next section, we take  $\varepsilon/b = 3.5$  and  $\mu/b = 3.8$ . The value of  $\varepsilon$  used is not very different from reported estimates of  $\varepsilon_{pd}$ , though these estimates vary over a wide range.

The value of the concentration  $p$  of oxygen vacancies in the plane is not known with accuracy better than  $\pm 1\%$  for any high-temperature superconductor. Experimental reports on samples claiming  $p$  is zero are not uncommon, but this limitation on the experimental resolution must be borne in mind. If it is definitively shown that high- $T_c$  superconductors exist with  $p = 0 \pm 10^{-4}$ , then this model

will have been shown to be irrelevant to the basic physics of the superconductivity. This does not appear to have occurred at present. In the calculations reported below, we mainly report results for the value  $p = 0.04$ , which is less than the value of 5%, which is the highest reported value<sup>16</sup> of which we are aware. We have made exploratory calculations on a range of  $p$  values up to 5%. The qualitative results are similar to those reported below as long as  $p$  is of the order of a few percent.

The value of  $J$  is completely unknown. We find that the mean-field model produces unphysical results when  $J$  is greater than about 2.0 (the exact upper limit depends on the other parameters), and we usually choose  $J = 1.5$  so that it is as large as possible while remaining in the physical region. This choice is made for computational convenience, because calculations with small  $J$  require very-long-time integrations, which are numerically very expensive. On the other hand, a  $J$  of order unity is not completely inconceivable physically: The  $J$  for the ordinary copper sites is known to be an extraordinarily large number of the order of 0.5 eV. Though the physics of the  $J$  in this model is quite different, this renders a value of order unity somewhat plausible. In fact,  $J$  could be substantially smaller and still yield a satisfactory  $T_c$  from an experimental point of view. The transition temperatures, however, cannot be taken seriously in comparison with experiments at this stage of model building in any case.

Finally, the physical picture in the Introduction requires that the Fermi level  $\mu$  be near the top of the (oxygenlike) band, so that the number of holes should be in the range of the characteristically small carrier hole densities observed in high- $T_c$  materials. We have studied the model for values of  $\mu$  in a range satisfying this criterion (usually  $\mu/b = 3.8$ ).

### RESULTS

We first present some results on the nature of the density of states in the normal state in the parameter ranges discussed in the last section. (The relevant parameters in the mean-field normal state are  $p$  and  $\varepsilon$ .  $J$  and  $\mu$  only affect the density of states at this mean-field level below  $T_c$ .) The total density of states is shown in Fig. 2 for

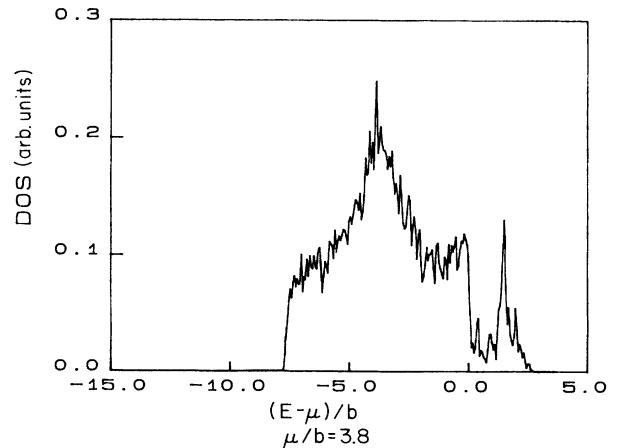


FIG. 2. Total normal-state density of states.

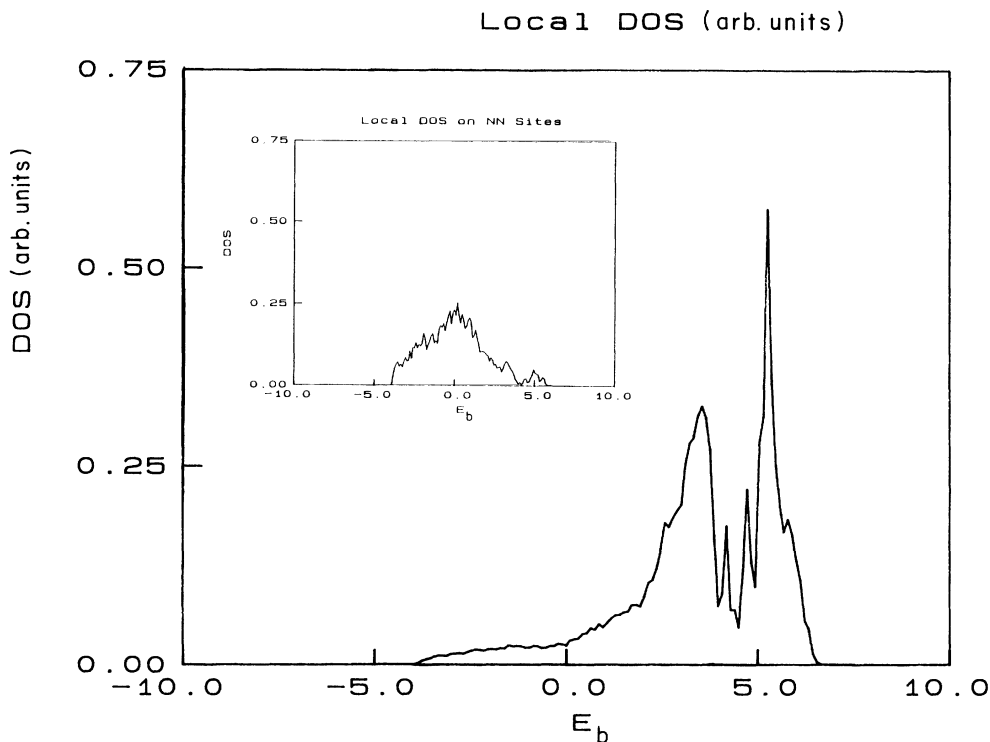


FIG. 3. Local density of states (a) at “special” sites adjacent to bonds with  $J_{ij} \neq 0$  and (b) at the next neighbors to these special sites as shown in the inset.

$\varepsilon=3.5$  and  $p=0.04$ . One sees that the presence of the special sites (interpreted as copper) next to the special bonds (oxygen vacancies) results in an extra peak at the top of the band. Looking at the local densities of states reveals the structure underlying this total state density. In Fig. 3 we show the average local density of states at the special (copper) sites and also at rings of sites equidistant from the special bonds, as indicated in the inset. One sees that there are *two* kinds of state at the special (“copper”) sites: The peak near the top of the total density of states is associated with a localized state, while there is a second peak in the local density of states for the special (“copper”) sites, which is associated with a resonance

lying inside the oxygen band and which is not localized. The qualitative picture of the anticipated nature of the paired superconducting state sketched in the Introduction would suggest that the kind of superconductivity we wish to study should occur when the Fermi level lies near, but slightly above the lower peak in the local density of states of the special sites.

We next report the density of states for self-consistent paired states, shown in Fig. 4 for  $\varepsilon/b=3.5$ ,  $p=0.04$ ,  $J/b=1.5$ , and  $\mu/b=3.8$ . In Fig. 5 we compare the region near the Fermi level with the corresponding result in the normal state. One sees some evidence of gaplike

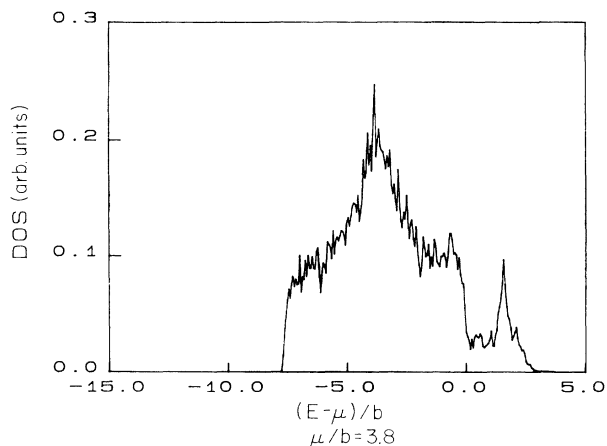


FIG. 4. Total density of states in superconducting state.

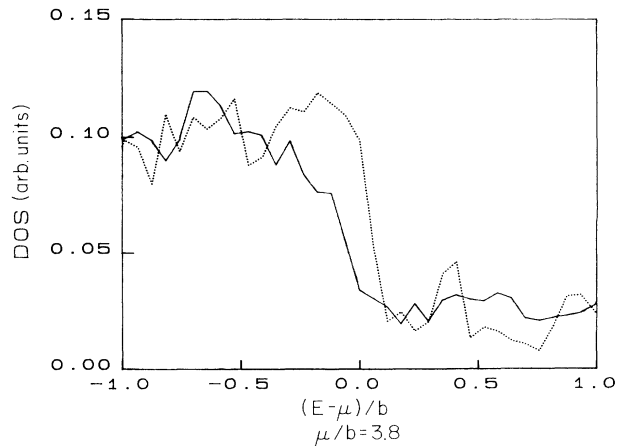
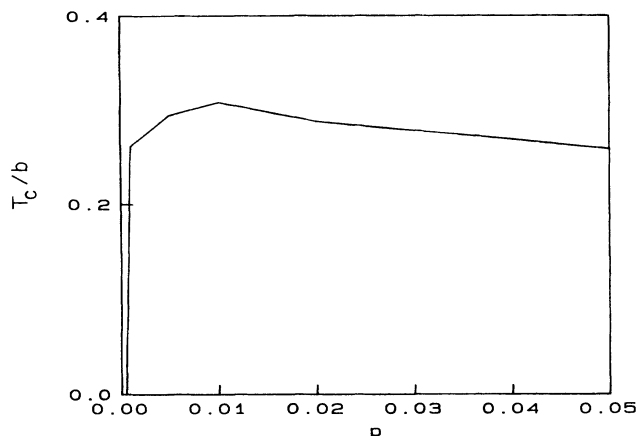


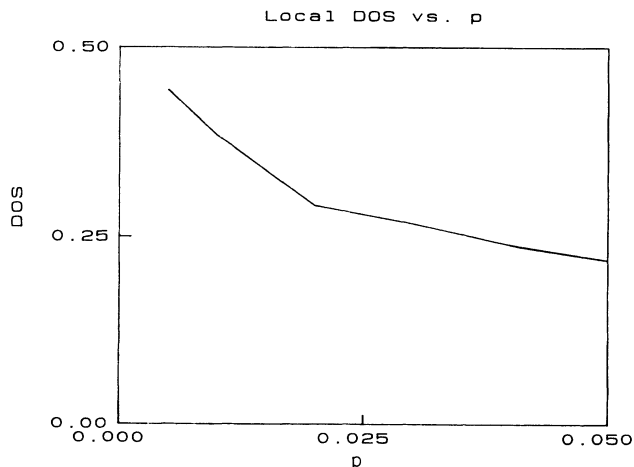
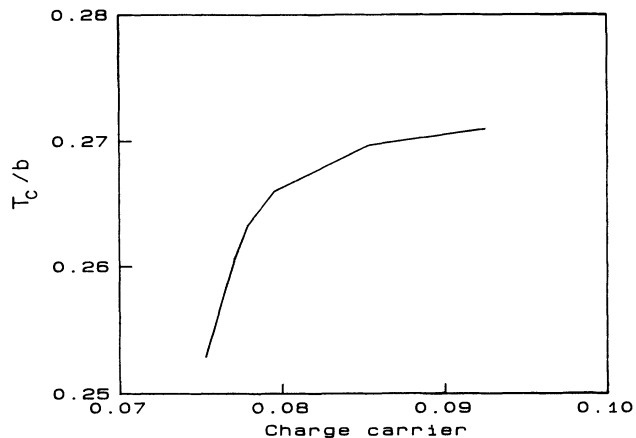
FIG. 5. Total density of states near the Fermi level in the superconducting (solid line) and normal states (dotted line).

FIG. 6.  $T_c(p)$  in the model.

structure, particularly if one looks at the local density of states at the special sites (discussed below: see Fig. 15). The gap is clearly not sharply defined, and there continues to be finite density of states at the Fermi level; that is, we have a “gapless” form of superconductivity.

We next report the systematics of  $T_c$  in the self-consistent solutions. In Fig. 6 we show  $T_c(p)$ . A striking feature is that we have a plateau in which  $T_c(p)$  is slowly varying (though decreasing) as  $p$  increases. The non-monotonicity of  $T_c$  as a function of  $p$  was at first quite surprising, since the physics clearly shows that  $T_c$  must be 0 when  $p \rightarrow 0$ . The local density of states at the Fermi level at the “copper sites” as a function of  $p$  is falling for increasing  $p$  (see Fig. 7). It appears that this effect is dominating the  $p$  dependence of  $T_c(p)$  in the region in which  $T_c(p)$  is dropping with increasing  $p$ . In Fig. 8 we show  $T_c$  as a function of hole concentration for the same set of parameters: If the Fermi level is in the band as discussed in the previous section, then  $T_c$  increases with carrier concentration.

The local charge density at the special sites is of interest, because it is believed to be related to the positron-

FIG. 7. Local density of states at the Fermi level as a function of  $p$ .FIG. 8.  $T_c$  as a function of carrier density.

annihilation rate for positrons trapped at vacancy sites.<sup>17-23</sup> We show this quantity as a function of temperature in Fig. 9.

A model for the effects of additional, nonmagnetic impurities on the superconductivity in this model has been described earlier.<sup>24</sup> Qualitatively, the expectation is that such nonmagnetic impurities should be more effective in destroying superconductivity than they would be in a model with a spatially uniform pairing force, because the nonmagnetic impurities can effectively act at the “weak links” between the regions of large pair correlations. To explore this effect with the present parametrization, we have found self-consistent solutions to the same BCS-like equations described in the previous section, in the case that the model is modified so that  $\epsilon_i$  takes three values: 0 at (“oxygen” sites, with probability  $1-2p-x$ ),  $\epsilon$  (at “copper” sites next to oxygen vacancies; as in the preceding section, these occur at the neighbors of “oxygen vacancies” occurring on the bonds of the lattice with probability  $p$ ) and  $\epsilon'$  (at “zinc” sites, distributed at random with site probability  $x$ ). The model thus differs from the one described in the preceding section only in the addition of randomly positioned sites with a value  $\epsilon'$  different from 0 or the value  $\epsilon$  assigned to “copper” sites next to

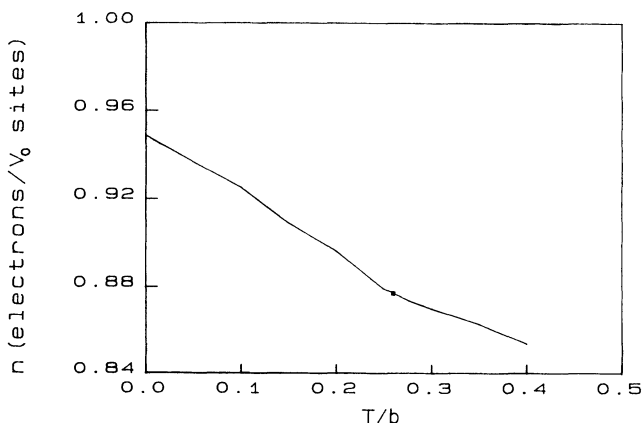


FIG. 9. Charge density at defects as a function of temperature.

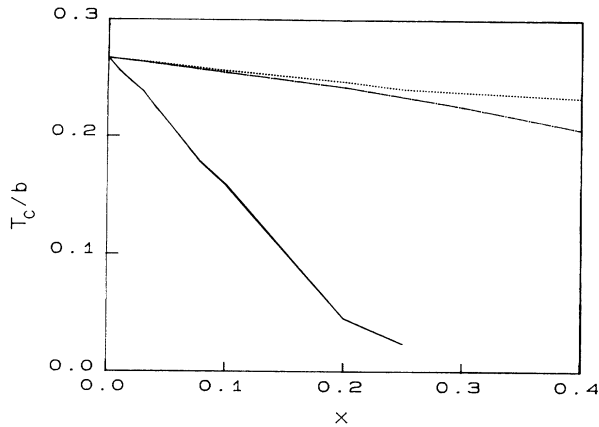


FIG. 10.  $T_c$  as a function of concentration  $x$  of added elastic impurities for models of homogeneous pairing [ $s$  (dashed line) and  $d$  (dotted line) waves] and heterogeneous [dilute,  $d$ -wave (solid line)] pairing.

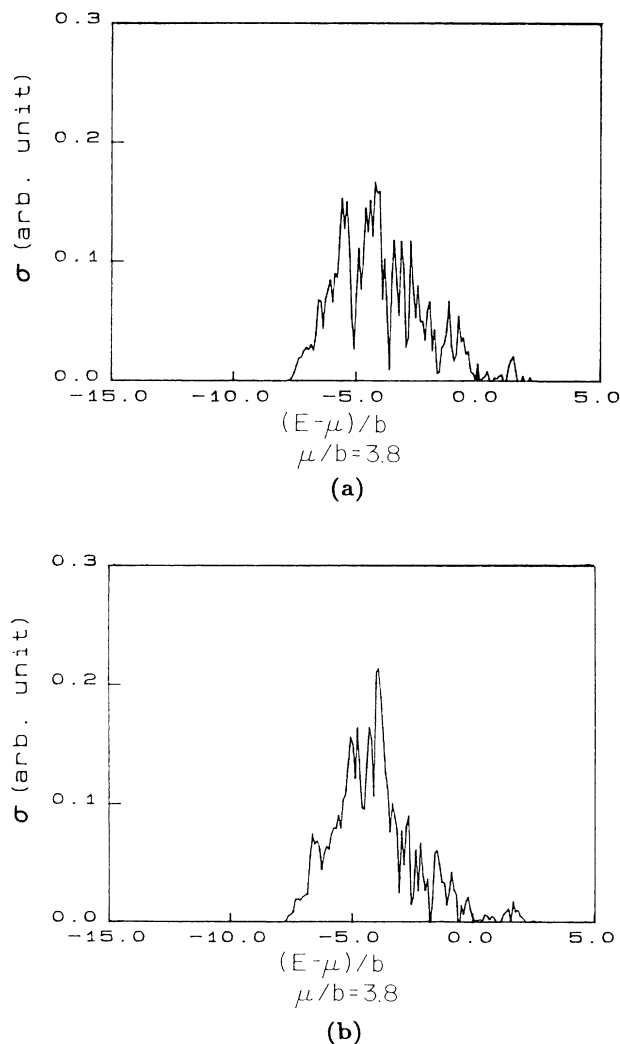


FIG. 11. dc conductivity as a function of the Fermi level energy in (a) the normal state and (b) the paired state.

oxygen vacancies. (In contrast, in Ref. 24, we used an Anderson model of continuously distributed values of  $\epsilon_i$  to describe the effects of other impurities.) Because  $x$  and  $p$  are both much less than 1 in the calculations we do, we neglect any possible effect of improbable sites which are both at the ends of “special” bonds and which are selected for the value  $\epsilon_i = \epsilon'$ . To establish that the conjectured effects of random heterogeneous distribution of the pairing force on the sensitivity of  $T_c$  to the “zinc” impurities, we also solved the BCS equation for a uniform pairing force in the same model, with  $J$  adjusted to give the same  $T_c$  at  $x=0$ . A few details of this control calculation are described in the Appendix. For  $\epsilon'$ , we used the value  $2.5/b$ . In Fig. 10 we show the effects of the added impurities on  $T_c$  in the case of  $s$ - and  $d$ -wave pairing in the case of homogeneous pairing and in the case of heterogeneous pairing with the parameters described in the previous section ( $\mu/b=3.8$ ). One sees in Fig. 10 that the result of the heterogeneous pairing model is to very sharply increase the sensitivity of  $T_c$  to the presence of on-site disorder of this type, as we conjectured and partly demonstrated earlier.

Finally, we show calculations of the zero-temperature conductivity in the normal and superconducting states in Fig. 11.

## CONCLUSIONS AND DISCUSSION

A first question about models of this sort is whether or not the required oxygen vacancies exist in the vast array of cuprate superconductors known experimentally. In this regard an important feature of the results is that a plateau appears in the calculations of  $T_c(p)$  (Fig. 6). This feature of the model renders it much more plausible physically, because it means that the approximate experimental reproducibility of  $T_c$  from sample to sample (in which the oxygen vacancy concentration certainly varies by a few percent) might not invalidate the present approach. Even granting this insensitivity to detailed oxygen-vacancy concentration, one may question whether the required oxygen-vacancy concentrations exist (though some reports<sup>16</sup> of the needed concentration of vacancies exist), given the many reports of zero oxygen-vacancy concentration in the plane. In this regard we point out that only a few percent of oxygen vacancies are required and that existing experimental methods do not determine oxygen-vacancy concentration to better than a few percent. It should be noted that the model refers to in-plane oxygen vacancies. Apical oxygen vacancies<sup>25</sup> might also play such a role. (In the case of compounds of the  $\text{La}_2\text{CuO}_4$  type, it is reported<sup>26</sup> that the large number of apical oxygen vacancies inferred in Ref. 25 might be vacancies in the copper oxygen plane, as postulated here, without altering the interpretation of that experiment.)

Vacancies in the chain planes of 1:2:3-type compounds almost certainly would not have the effects required for the present model. Experimentally, of course, one produces superconductivity in 1:2:3 compounds by adding oxygen to the chain planes. This would not contradict the assumptions of the present model if we imagine that adding oxygen in the chain planes may drive some oxy-

gen off the superconducting copper oxygen sheets, producing the in-plane oxygen vacancies required in the model. Such a hypothesis could be tested by Madelung energy calculations, which we have not undertaken. Point-defect energy calculations have been undertaken by Baetzold.<sup>27</sup> In  $\text{YBa}_2\text{Cu}_3\text{O}_7$ , he reports vacancy-formation energies for oxygen sites 1 (chain plane), 4 (apical), 2, and 3 (sheets) of 17.23, 17.34, 21.90, and 21.76 eV, respectively. More importantly, however, he reports the considerably lower energy of 1.19 eV for formation of a Frenkel defect in which the oxygen at site 1 in the chain plane is moved to the oxygen at site 5, also in the chain plane. The hypothesis discussed in this paragraph postulates the (probably nonequilibrium) formation of Frenkel defects in which an oxygen at site 2 or 3 is moved to site 5. No calculation of the energy cost of such a Frenkel defect is reported in Ref. 27.

There is one set of experiments which bear rather directly on the question of the existence and superconductive relevance of oxygen vacancies of the postulated sort: These are measurements of positron-annihilation rates which exhibit a positron-decay rate associated with positrons trapped at oxygen vacancies. For some time experiments have existed<sup>17-23</sup> which showed that a kink

exists at  $T_c$  in the temperature dependence of this annihilation rate. The annihilation rate is in turn proportional to the electron density at the trapping site. In one paper<sup>23</sup> the measured rates were converted to a local electron density at the vacancy, as shown in Fig. 12(a). In Fig. 12(b) we show a calculation of the temperature dependence of the local charge density as calculated in the model with the same parameters used for most of the other calculations reported here ( $\mu/b=3.8$ ,  $p=0.04$ ,  $\epsilon/b=3.5$ ,  $J/b=1.5$ ). A kink occurs at  $T_c$ , as qualitatively expected in this model, in which the phase transition produces increased phase coherence of the order parameter at the special "oxygen-vacancy" sites. The scale of  $T_c$  is unrealistic, but one sees that in other respects the temperature dependence of the calculated local charge density is in semiquantitative agreement with this experimental data on  $\text{YBa}_2\text{Cu}_3\text{O}_{7-x}$  (YBCO). Other investigators see similar effects in positron annihilation in YBCO, but in  $\text{La}_{2-x}\text{Sr}_x\text{CuO}_4$  and the thallium compounds, the reported effect of superconductivity on the positron lifetime has the opposite sign. These variations in the sign of the positron-annihilation lifetime effect in various high- $T_c$  materials may be associated with differences in the trapping behavior of the positrons in these materials.

The postulated existence in this model of a spatially heterogeneous pairing force provides a possible qualitative explanation of the otherwise mysterious fact that  $T_c$  is anomalously sensitive to nonmagnetic impurities. Elsewhere<sup>24</sup> we pointed out that our model would lead to a strong sensitivity of the superconductivity to nonmagnetic substitutional point defects, as observed experimentally, because the point defects will have a large effect on the coupling between regions of strong superconducting correlations near the "pairing centers" associated with oxygen vacancies. In Fig. 13(a) we show experimental data<sup>28</sup> on  $T_c$  as a function of substitutional concentration for a number of cationic substituents for copper in YBCO, and in Fig. 13(b) we show the corresponding calculation in the model as discussed in the preceding section. The trends are quite strikingly similar, and (Fig. 10)  $T_c$  is much more sensitive to spin-independent elastic scatterers than it is in a model with uniform pairing forces. [Because we have used an artificially large value of  $J$  for numerical reasons, the magnitudes of  $T_c$  in Fig. 13(b) are unrealistically large.] No fine tuning of the parametrization of the model was made to produce the result in Fig. 13(b).

We note that the model qualitatively predicts that, at fixed  $p$  ("oxygen-vacancy" concentration), varying the carrier concentration (controlled by  $\mu$  in this model) can be expected to lead, as  $\mu$  increases, to a rise in  $T_c$  as  $\mu$  comes into resonance with the available level on the "Cu<sup>1+</sup>" sites next to the special bonds ("oxygen vacancies") as controlled by  $\epsilon$  in the model and then to a fall as  $\mu$  moves far above this level. Such a rise and fall of  $T_c$  with carrier concentration does occur, of course, in all high- $T_c$  materials, though it could have several origins, and it is by no means clear that the oxygen vacancy concentration in the plane remains fixed as the carrier concentration is varied. Nevertheless, we made such a calculation within the model, varying  $\mu$  around the value

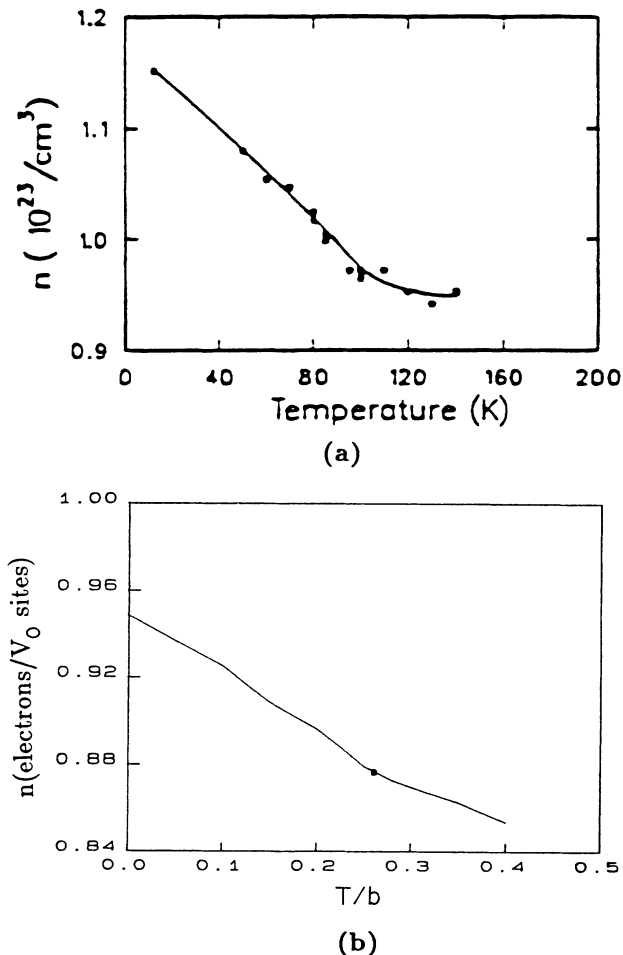


FIG. 12. Comparison of (a) the local electron density deduced from positron-annihilation-rate measurements (Ref. 23) in YBCO with (b) mean-field calculation in the dilute  $t$ - $J$  model.



3.8*b* used elsewhere in these calculations and fixing the other parameters ( $p=0.04$ ,  $J/b=1.5$ ,  $\epsilon/b=3.5$ ), with results shown in Fig. 14(b), for comparison with experiments on  $T_c$  as a function of carrier concentration [as determined from Hall-effect measurements<sup>29</sup> on thin films of  $\text{DyBa}_2\text{Cu}_3\text{O}_{7-\delta}$  (DBCO)] as shown in Fig. 14(a). Here, again, the results are qualitatively quite similar to the experimental ones, and we stress that no special adjustments were made to fit the data.

In principle, the model could also be tested by comparison with the vast array of spectroscopic experimental results that exist. Since the model can only be expected at best to describe the low-energy physics, we cannot anticipate any of the relatively high-energy photoemission results to be relevant. It would be of interest to compare calculated optical conductivity in the infrared region with experiments, and we have begun such calculations using the methods of the previous section, but they are very expensive, since the results are strongly affected by localization effects and require very long computational times to average over large fluctuations. At present, we

only report a comparison with tunneling data, which, in principle, measures the more easily calculable density of states on the appropriate energy scale. Unfortunately, it is well known that tunneling experiments present special difficulties in the high- $T_c$  materials.<sup>30,31</sup> As a result, these experiments show tremendous variation from one experiment to another. In the type of model considered here, this variation itself might find partial explanation in the spatial heterogeneity, which leads to wide variations in the local density of states [compare Figs. 3 and 2]. Further, we note that this model does give a rising density of states away from the Fermi energy (Fig. 5), reminiscent of the V-shaped density observed in many experiments and the subject of many theoretical speculations. In this model this feature arises because the Fermi surface was assumed to lie near the top of the conduction band, with a localized state associated with the copper sites near oxygen vacancies lying above it. With regard to "gaplike" structure, we see evidence in the density of states of a

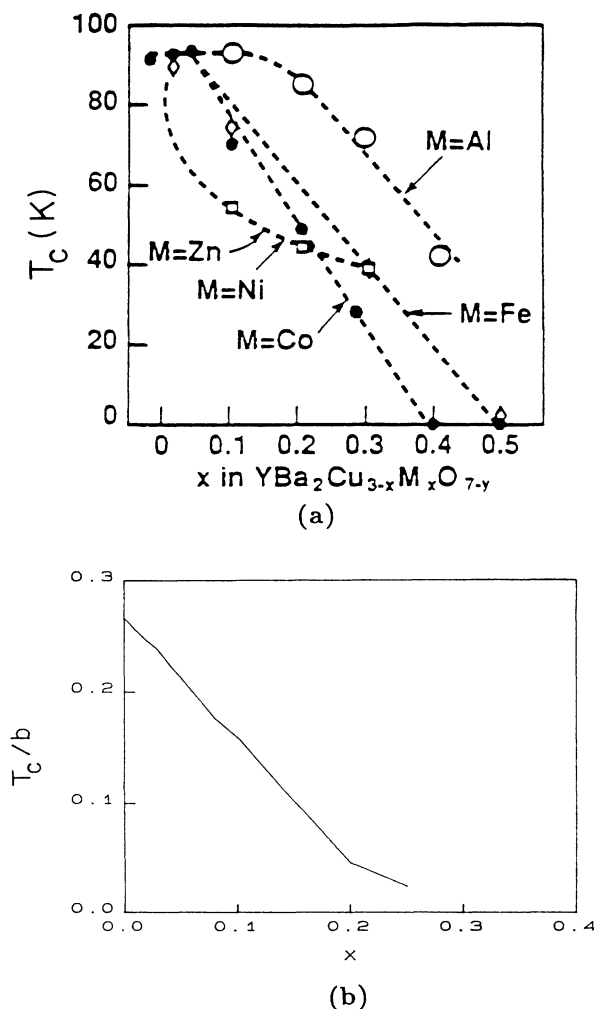


FIG. 13. Comparison of (a)  $T_c$  as a function of cationic substituent concentration  $x$  (Ref. 28) in YBCO with (b) mean-field calculations in the dilute  $t$ - $J$  model.

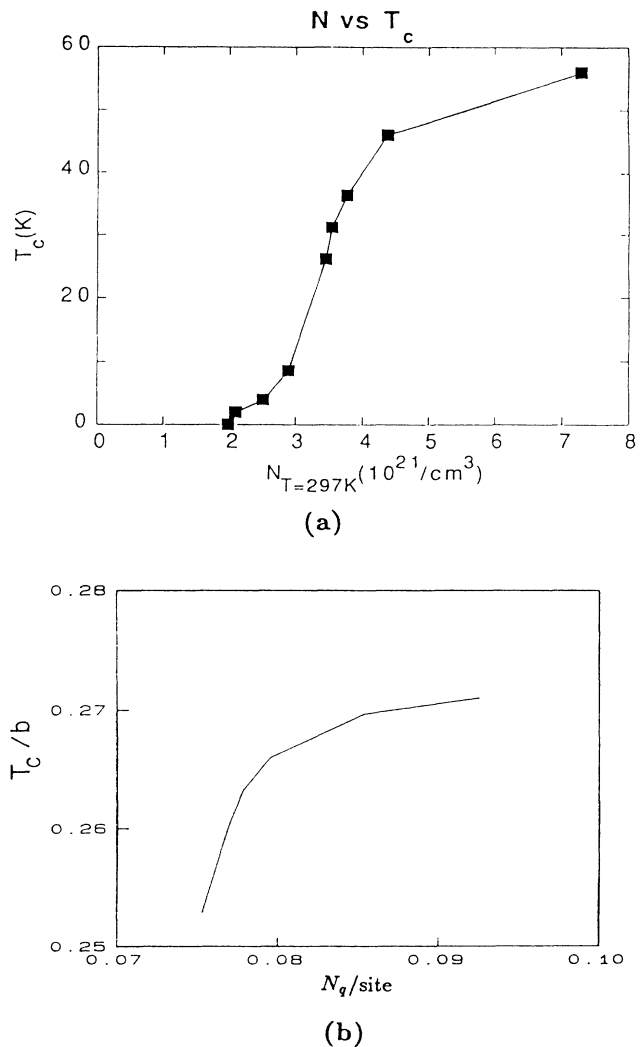


FIG. 14. Comparison of (a) measured  $T_c$  as a function of measured inverse Hall conductivity (Ref. 29) in DBCO with (b) mean-field calculation of  $T_c$  as a function of carrier concentration in the dilute  $t$ - $J$  model.

superficially gaplike structure in the normal-state density of states, though this is not connected with the correlations in the electron system in any direct way. In the mean-field BCS state (Fig. 5), this gaplike structure is actually less in evidence than it is in the normal state. There are very few measurements of the temperature dependence of the tunneling conductance. In Ref. 32 the peaks which the authors associated with the gap did not change position with temperature, in qualitative agreement with our result. To give a more definite idea of how the calculated densities of states compare with those measured in tunneling experiments, we show some experimental data on YBCO from Ref. 30 in Fig. 15(a) and compare it with a calculation of the local density of states (DOS) at the special ("oxygen-vacancy") sites on a very roughly similar energy scale in Fig. 15(b). These results look somewhat similar, but the comparison must be treated quite cautiously. In particular, the calculated total density of states has much less structure than the local one, and calculations at higher-energy resolution show even more structure at finer energy scales, which we do not fully understand.

Among several other properties of the superconducting state which it would be interesting to calculate in this model are the nuclear relaxation rate  $T_1$  and the acoustic attenuation, which behave differently as a function of temperature than they do in ordinary BCS superconductors. There seems to be a possibility that the strong disorder in this model would significantly alter the delicate interference effects which lead to the BCS predictions in the more familiar case.

We believe that there is a possibility that a model along the present lines might account for the unusual normal-state properties of high-temperature superconductors. The physical argument is that, above  $T_c$ , pairing correlations are expected to remain locally very strong around the pairing centers, but these correlations will be phase incoherent with similar correlations around other point-defect pairing centers. If the temporal spectrum of the corresponding phase fluctuations is essentially flat over thermal energies, then it appears that these fluctuations would have many of the properties required by the marginal-Fermi-liquid theory for explaining the normal-state properties.<sup>33</sup>

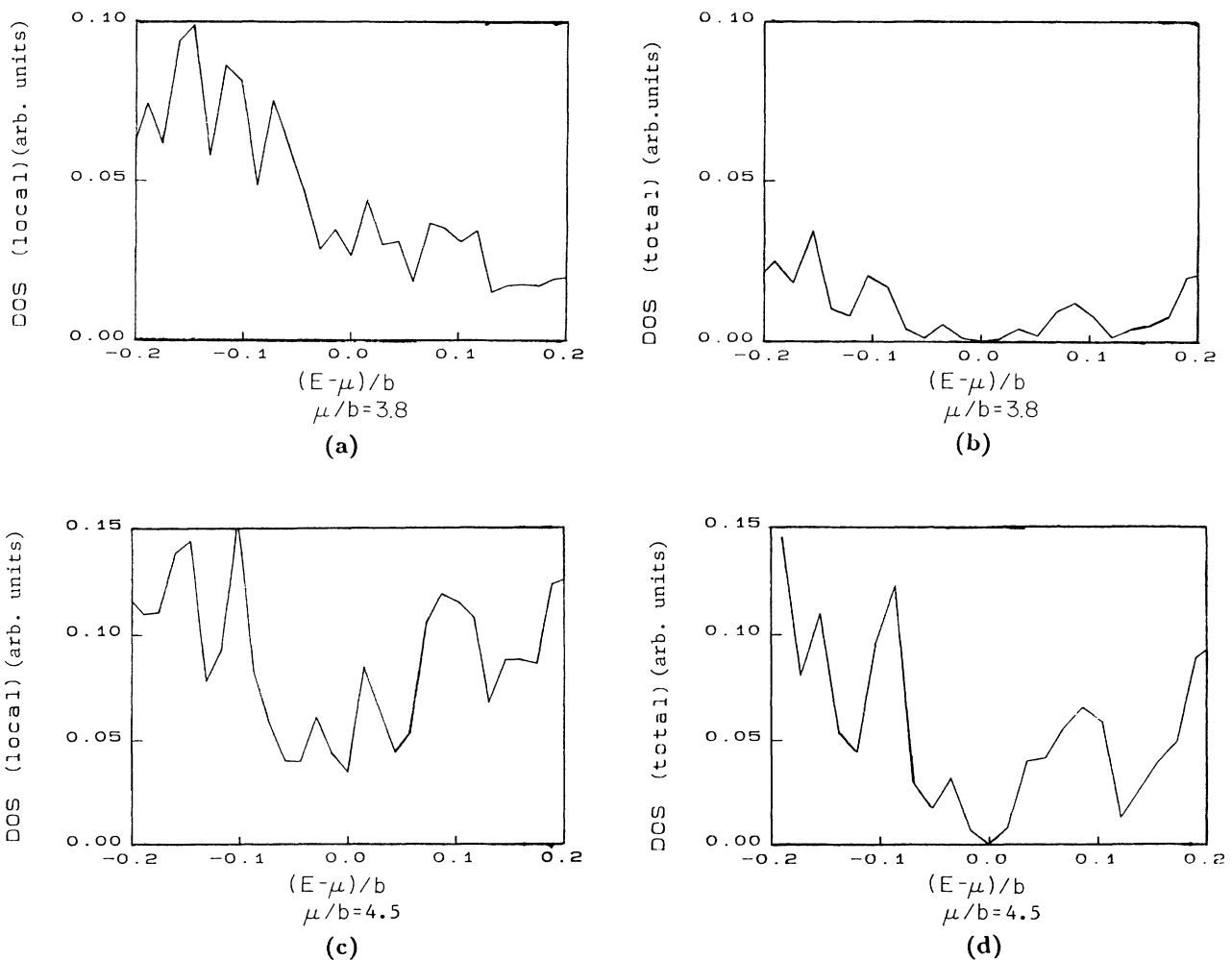


FIG. 15. Various DOS in the neighborhood of the Fermi level in the pairing state in the dilute  $t$ - $J$  model: (a) Total DOS and (b) local DOS with Fermi level below, but close to the top of the band ( $\mu/b = 3.8$ ). (c) Total DOS and (d) local DOS with Fermi energy  $\mu/b = 4.5$  lying above the band edge.

Ideas somewhat similar to those discussed here have been put forward by Phillips and Rabe<sup>7,34-37</sup> and Bar-Yam.<sup>38</sup> In the first case, the proposed defect-induced mechanism is phonon related, whereas we suppose that the pairing mechanism is of electronic origin. In the work of Phillips and Rabe, the nature of the defects is not discussed very specifically and detailed calculations including disorder are lacking. Bar-Yam proposes oxygen vacancies as an essential feature of an electronic pairing mechanism. His detailed calculations neglect disorder altogether. Many of the qualitative features of the model which we have discussed depend specifically on the disorder.

Clearly, a complete theory based on a model of this type must also take into account the interaction of the holes with the copper spins away from oxygen vacancies, which is presumed by many theorists (but not by us) to contain the essential physics leading to superconductivity.

The model studied here is clearly very schematic, when compared with the real high- $T_c$  materials. Further, the mean-field approximation employed is naive, though we do take exact account of the one-electron effects of disorder. Nevertheless, the results seem to hold some promise. In particular, one may get a qualitative picture suggesting explanations of many surprising features of high-temperature superconductors from this model.

#### ACKNOWLEDGMENTS

We have benefited from discussions with many people including R. Joynt, H. B. Shore, S. Sen, C. Dasgupta, A. Goldman, T. V. Ramakrishnan, and T. F. Wang. We are grateful for a grant from the Electric Power Research Institute and for support from the Minnesota Supercomputer Institute.

#### APPENDIX:

##### BCS THEORY FOR A UNIFORM PAIRING FORCE

It is a standard exercise to write down the gap equation for the Hamiltonian (1) when  $J_{ij}$  is a constant value for nearest neighbors and zero otherwise,  $b_{ij}=b$  for nearest neighbors, and  $\epsilon_i$  and  $\mu$  are constants. Defining

$$d_{q,\sigma} = \frac{1}{\sqrt{N}} \sum_i d_{i,\sigma} e^{-iq \cdot r_i}, \quad (\text{A1})$$

one finds (see, for example, Ref. 39), at finite temperatures,

$$\Delta_q = -\frac{1}{2} \sum_{q'} \frac{V_{q,q'} \Delta_{q'}(T) \tanh[\mathcal{E}(T, q')/2k_B T]}{[\Delta_{q'}^2 + E_{q'}^2]^{1/2}}, \quad (\text{A2})$$

in which

$$V_{q,q'} = -4J \sum_{\delta} \cos(\mathbf{q} \cdot \delta) \cos(\mathbf{q}' \cdot \delta) \quad (\text{A3})$$

and

$$E_{q,q'} = \epsilon - \mu - 2b \sum_{\delta} \cos(\mathbf{q}' \cdot \delta), \quad (\text{A4})$$

while

$$\mathcal{E}(T, \mathbf{q}) = [E_q^2 + \Delta_q(T)^2]^{1/2}. \quad (\text{A5})$$

We consider  $s$ - and  $d$ -wave solutions for (A2):

$$\Delta_q^{(s,d)}(T) = 2\Delta^{(s,d)}[\cos(q_x a) \pm \cos(q_y a)]. \quad (\text{A6})$$

For  $s$ -wave solutions the Fermi level was chosen at the center of the band ( $\mu=0$ ), whereas for  $d$ -wave solutions we took  $\mu/b=3.8$  in order to obtain approximately the observed number of carriers. For the  $s$ -wave calculation  $\epsilon_i$  was taken as  $-0.3b$ , whereas for the  $d$ -wave calculation we took  $\epsilon_i/b=3.5$ . In the control calculation described in the text,  $J$  in this uniform pairing force model was adjusted in order to obtain transition temperatures from (A2) which were the same as those found in the dilute model. The required values of  $J/b$  were 1.405 ( $d$  wave) and 0.82 ( $s$  wave). Then elastic-scattering impurities were added to the model, and  $T_c$ 's were found as a function of their concentration  $x$  using equation-of-motion methods, with results shown in Fig. 10.

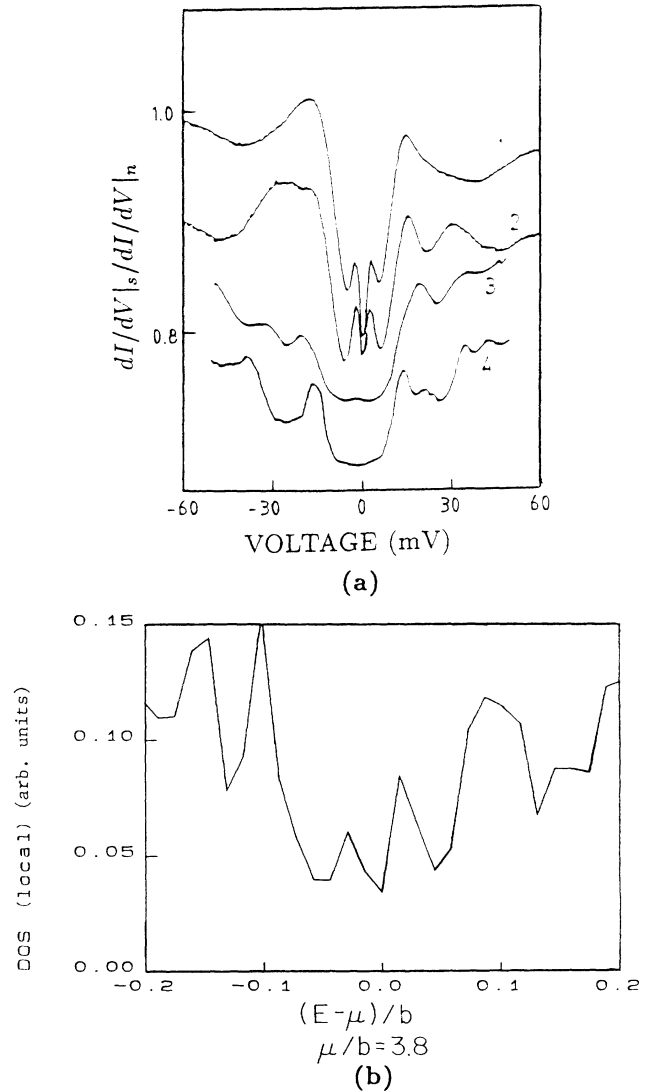


FIG. 16. (a) Tunneling density-of-states measurements (Ref. 30) compared with (b) calculation of the local DOS at special bonds in the dilute  $t$ - $J$  model.

- <sup>1</sup>J. G. Bednorz and K. A. Müller, *Z. Phys. B* **64**, 189 (1986).
- <sup>2</sup>M. K. Wu, J. R. Ashburn, C. J. Torng, P. H. Hor, R. L. Meng, L. Gao, Z. J. Huang, Y. Q. Wang, and C. W. Chu, *Phys. Rev. Lett.* **58**, 908 (1987).
- <sup>3</sup>J. D. Jorgensen, *Phys. Today* **44**(6), 34 (1991).
- <sup>4</sup>A. Sleight, *Phys. Today* **44**(6), 24 (1991).
- <sup>5</sup>*Oxygen Disorder Effect in High  $T_c$  Superconductors*, edited by J. L. Morán-López and I. Schuller (Plenum, New York, 1990).
- <sup>6</sup>J. W. Halley and H. B. Shore, *Phys. Rev. B* **37**, 525 (1988).
- <sup>7</sup>J. C. Phillips, *Phys. Rev. Lett.* **59**, 1856 (1987).
- <sup>8</sup>J. W. Halley, S. Davis, P. Samsel, and R. Joynt, *Bull. Mater. Sci. (India)* **14**, 1069 (1991).
- <sup>9</sup>J. W. Halley, C. Das Gupta, S. Davis, and X-F. Wang, in *Proceedings of Many Body VII* (Plenum, New York, in press).
- <sup>10</sup>For example, A. J. Arko *et al.*, *Phys. Rev. B* **40**, 2268 (1989).
- <sup>11</sup>For example, R. V. Kasowski, W. Y. Hsu, and F. Herman, *Phys. Rev. B* **36**, 7248 (1987).
- <sup>12</sup>R. Haydock, V. Hene, and M. J. Kelly, *J. Phys. C* **5**, 2845 (1972).
- <sup>13</sup>D. Weaire and E. P. O'Reilly, *J. Phys. C* **18**, 1401 (1985).
- <sup>14</sup>J. W. Halley, H. B. Shore, and N. Tit (unpublished).
- <sup>15</sup>G. D. Mahan, *Many Particle Physics* (Plenum, New York, 1981), pp. 823–827.
- <sup>16</sup>M. A. Beno, L. Soderheim, D. W. Capone II, D. G. Hinks, J. D. Jorgensen, J. D. Grace, I. K. Schuller, C. U. Segre, and K. Zhang, *Appl. Phys. Lett.* **51**, 57 (1987).
- <sup>17</sup>Y. C. Jean, S. J. Wang, H. Nakanishi, W. N. Hardy, M. Y. Hayden, R. F. Keifl, R. L. Meng, P. H. Hor, Z. J. Huang, and C. W. Chu, *Phys. Rev. B* **36**, 3994 (1987).
- <sup>18</sup>Y. C. Jean, J. Kyle, H. Nakanishi, P. E. A. Turchi, R. H. Howell, A. L. Wachs, M. J. Fluss, R. L. Meng, P. H. Hor, Z. J. Huang, and C. W. Chu, *Phys. Rev. Lett.* **60**, 1069 (1988).
- <sup>19</sup>Y. C. Jean, H. Nakanishi, M. J. Fluss, A. L. Wachs, P. E. A. Turchi, R. H. Howell, Z. Z. Wang, R. L. Meng, P. H. Hor, Z. J. Huang, and C. W. Chu, *J. Phys. Condens. Matter* **1**, 2696 (1989).
- <sup>20</sup>Y. C. Jean *et al.*, *Phys. Rev. Lett.* **64**, 1593 (1990).
- <sup>21</sup>D. R. Harshman, L. F. Schneemeyer, J. V. Wasczak, Y. C. Jean, M. J. Fluss, R. H. Howell, and A. L. Wachs, *Phys. Rev. B* **38**, 848 (1988).
- <sup>22</sup>E. C. von Stetten, S. Berko, S. S. Li, R. R. Lee, J. Brynstead, D. Singh, H. Krakauer, W. E. Pickett, and R. E. Cohen, *Phys. Rev. Lett.* **60**, 2198 (1988).
- <sup>23</sup>S. G. Usmar, P. Sferlazzo, K. G. Lynn, and A. R. Moodenbaugh, *Phys. Rev. B* **36**, 8854 (1987).
- <sup>24</sup>J. W. Halley, S. Davis, and S. Sen, *Physica B* **165&166**, 999 (1990).
- <sup>25</sup>E. Tan, M. E. Filipkowski, J. I. Budnick, E. K. Heller, D. L. Brewe, B. L. Chamberland, C. E. Bouldin, J. C. Woicik, and D. Shi, *Phys. Rev. Lett.* **64**, 2715 (1990).
- <sup>26</sup>J. I. Budnick (private communication).
- <sup>27</sup>R. Baetzold, *Physica C* **181**, 252 (1991).
- <sup>28</sup>J. M. Tarascon and B. G. Bagley, in *Chemistry of Superconductor Materials*, edited by T. A. Vanderah (Noyes, Park Ridge, NJ, 1992), Chap. 8, p. 310.
- <sup>29</sup>T. Wang, K. M. Beauchamp, D. D. Berkley, B. R. Johnson, J. X. Liu, T. Zhang, and A. M. Goldman, *Phys. Rev. B* **43**, 8623 (1991).
- <sup>30</sup>J. R. Kirtley, *Int. J. Mod. Phys. B* **4**, 201 (1990).
- <sup>31</sup>J.-X. Liu, J.-C. Wan, A. M. Goldman, Y. C. Chang, and P. Z. Jiang, *Phys. Rev. Lett.* **67**, 2195 (1991).
- <sup>32</sup>J. Geerk, X. X. Xi, and G. Linker, *Z. Phys. B* **73**, 329 (1988).
- <sup>33</sup>C. M. Varma, P. B. Littlewood, S. Schmitt-Rink, E. A. Abrahams, and A. Rickenstein, *Phys. Rev. Lett.* **63**, 1996 (1989).
- <sup>34</sup>J. C. Phillips, *Phys. Rev. Lett.* **64**, 1605 (1990).
- <sup>35</sup>J. C. Phillips, *Phys. Rev. B* **41**, 8968 (1990).
- <sup>36</sup>J. C. Phillips, *Phys. Rev. B* **43**, 6257 (1991).
- <sup>37</sup>J. C. Phillips and K. M. Rabe, *Phys. Rev. B* **44**, 2863 (1991).
- <sup>38</sup>Y. Bar-Yam, *Phys. Rev. B* **43**, 359 (1991); **43**, 2601 (1991).
- <sup>39</sup>J. Callaway, *Quantum Theory of the Solid State* (Academic, San Diego, CA, 1974), pp. 665–676.